

CRACK GROWTH UNDER ALTERNATING LOADING

V. M. Tikhomirov

UDC 620.178.6

Crack propagation under alternating loading is investigated. Relations between the growth rate of a fatigue defect and loading parameters and the expression for the stress intensity factor are derived for compression of a cracked solid taking into account the possible contact of the crack faces. A model for the deformation of a small region near the crack tip is proposed which allows one to formulate the conditions of residual opening of a growing fatigue crack. The experimental data obtained in tests of steel samples are compared with the results of calculation using the developed procedure.

Key words: *alternating loading, fatigue crack, initial crack opening, stress intensity factor.*

Introduction. In the analysis of fatigue crack growth, it is customary to use kinetic diagrams of material fracture, in which experimental results are represented in the form of dependences of crack growth rate on the amplitude of the stress intensity factor (SIF). The diagrams have three characteristic segments corresponding to different mechanisms of crack growth.

The first segment, whose beginning corresponds to the threshold value of the SIF, is characterized by a low crack growth rate. In the range of moderate rates of crack extension (the second segment), the experimental data are well described by the Paris formula

$$\frac{dl}{dN} = C(\Delta K_I)^m, \quad (1)$$

where l is the length of the growing crack, N is the number of loading cycles, and ΔK_I is the SIF amplitude, and C and m are constant coefficients. The third segment corresponds to high rates and unstable crack growth as the maximum value of the SIF approaches its critical value.

A large number of theoretical and empirical expressions have been proposed to describe fracture diagrams. However, there is no generally accepted approach to describing the fatigue fracture mechanism in metals. Existing theoretical models can be divided into two groups [1]:

- models using the crack-face opening or other deformation criteria;
- models based on integrated criteria: Total plastic strain, total energy of plastic deformation or total fatigue damage to material.

Relation (1), included in the first group, was obtained under the assumption that the crack growth rate depends on the plastic strain amplitude $\Delta\varepsilon_p$ for one loading cycle. This dependence correlates with the Coffin–Manson law [2]:

$$N_f = C_1(\Delta\varepsilon_p)^{C_2}.$$

Here N_f is the number of loading cycles of a smooth sample before fracture and C_1 and C_2 are coefficients which are constant for the material studied.

The Paris formula is used to describe crack propagation under both cyclic extension and alternating loading. In the latter case, it is assumed that the compression phase does not influence crack propagation; therefore, irrespective of the value of the compressive loads, a semblance of pulsating loading is considered. However, from

Siberian State University of Means of Communication, Novosibirsk 630049; twm@stu.ru. Translated from *Prikladnaya Mekhanika i Tekhnicheskaya Fizika*, Vol. 49, No. 5, pp. 190–198, September–October, 2008. Original article submitted March 26, 2007; revision submitted August 10, 2007.

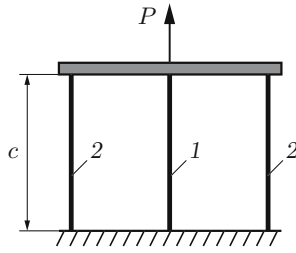


Fig. 1. Elastoplastic rod model: 1) ideally plastic rod; 2) absolutely elastic rod.

an analysis of experimental data [3], it follows that the crack propagation rate depends greatly on the value of compressive cyclic loads. The initiation and propagation of fatigue defects directly in the field of the stress arising from cyclic compression was also observed [4].

In the present paper, we consider a procedure that allows an analysis of crack propagation under alternating loading taking into account fatigue growth in compression half-cycles.

1. Modeling Elastoplastic Cyclic Deformation of the Region near the Crack Tip. In the vicinity of the tip of a fatigue crack propagating in metals, a plastic zone forms in which cyclic deformation leads to the accumulation of defects. To qualitatively describe the stress-strain state of the small volume at the tip of a growing crack, we use the rod model. The material in the examined region is considered ideally plastic and cyclically stable. Figure 1 shows the proposed rod model. The central ideally plastic rod models the small volume of the material located in the prefracture zone. The two symmetrically located rods model the elastoplastic material surrounding the region of plastic flow. The displacement δ of the horizontal absolutely rigid rod of the system corresponds to the crack tip opening. As a first approximation, the quantity δ can be assumed to depend on the SIF [2]:

$$\delta = K_I^2 / (E\sigma_y) \quad (2)$$

(E and σ_y are the elastic modulus and the yield limit of the material, respectively).

The rod system is loaded by force P which changes cyclically in time: $P = P_a \sin(\omega t) + P_m$ (ω is the loading frequency). For simplicity, the geometrical parameters of all elements are considered identical: the cross-sectional area of each rod is A and the length is c .

The maximum load level is chosen from the condition of return flow which is observed in the vicinity of the crack tip during unloading. In [2], this condition is formulated as follows: the plastic compression strain (return flow) during unloading corresponds to the plastic strain during extension if the yield point of the material increases by a factor of two. For the rod system considered, this condition is satisfied for

$$P_{\max} = 9\sigma_y A. \quad (3)$$

Let us compare the elastoplastic deformation of the central rod for symmetric loading cycle (amplitude of the cycle is $P_a = P_{\max}$ and average value is $P_m = 0$) and pulsating loading cycle ($P_a = P_m = P_{\max}/2$).

Figure 2 shows the strain diagram corresponding to the symmetric cycle. We consider in more detail the operation of the rod system in this loading regime.

In view of relation (3), plastic flow begins under load $P_1 = P_{\max}/3$ and displacement $\delta_1 = \sigma_y c/E$ (point 1 in Fig. 2). An increase in the load to $P_2 = P_{\max}$ (point 2) does not influence the stress in the central rod, and its strain increases to $\delta_2 = 4\sigma_y c/E$. With further unloading to the force $P_3 = P_{\max}/3$ (point 3), the stress reaches the yield limit in compression ($\sigma = -\sigma_y$) and the strain decreases: $\delta_3 = 2\sigma_y c/E$. Return flow of the material (the segment between points 3 and 4) begins; in this case, $P_4 = -P_{\max}/3$ and $\delta_4 = \sigma_y c/(2E)$. Plastic deformation of the central element continues up to the attainment of the maximum compressing load $P_5 = -P_{\max}$ (point 5); in this case, $\delta_5 = -4\sigma_y c/E$. The subsequent unloading occurs in two stages: 1) elastic deformation of the central rod, which corresponds to the segment between points 5 and 6 in Fig. 2 ($P_6 = -P_{\max}/3$ and $\delta_6 = -2\sigma_y c/E$); 2) plastic flow, which corresponds to the segment between points 6 and 7 [$P_7 = 0$ and $\delta_7 = -\sigma_y c/(2E)$].

The beginning of the second loading cycle is accompanied by plastic deformation of the rod; in this case, the maximum load in the diagram corresponds to point 8, which coincides with point 2 (Fig. 2b). The further deformation of the rod proceeds in a closed cycle. The plastic strain amplitude for one loading cycle is equal to $\Delta\varepsilon_p = 6\sigma_y/E$.

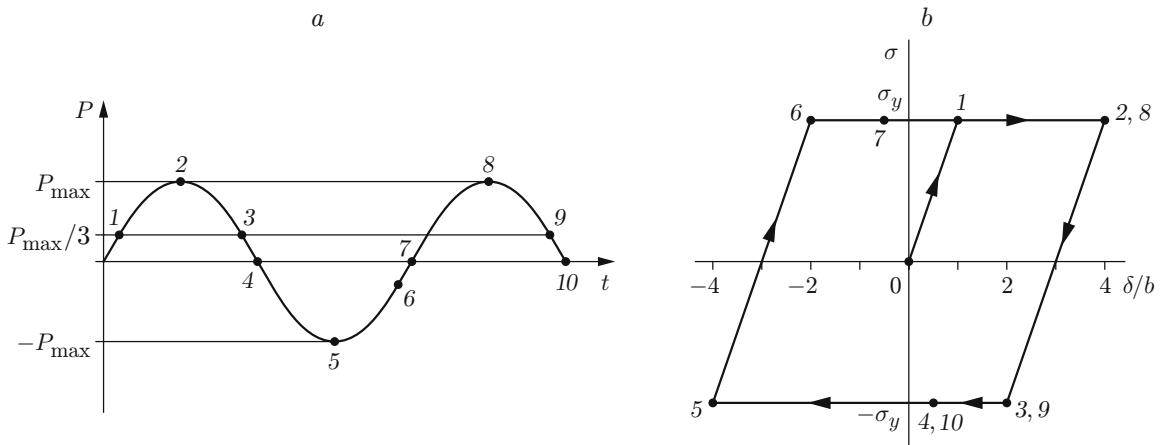


Fig. 2. Load variation (a) and a strain diagram of an ideally plastic element (b) in a symmetric loading cycle ($b = \sigma_y c/E$).

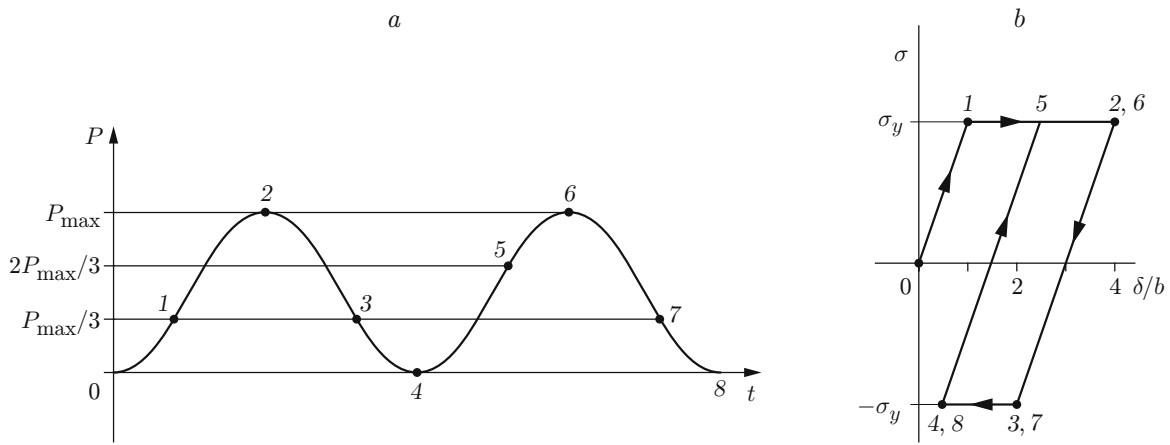


Fig. 3. Load variation (a) and a strain diagram of an ideally plastic element (b) under pulsating loading.

Figure 3 shows a strain diagram for pulsating loading. In this case, $\Delta\varepsilon_p = 3\sigma_y/(2E)$.

Thus, in the symmetric loading cycle, the value of $\Delta\varepsilon_p$ is four times larger than that in the pulsating cycle. At the same time, with the compression phase taken into account, the stress intensity factor amplitude is twice larger. This allows the use of a power-law dependence similar to the Paris formula to calculate the fatigue crack growth rate:

$$\frac{dl}{dN} = C(K_I^t + K_I^c)^m \quad (4)$$

(K_I^t and K_I^c are the SIF values for the maximum extension and compression, respectively). In the calculation of the SIF K_I^c , it is necessary to take into account the possible contact of the crack faces.

2. Compressive Stress Intensity Factor. Let, in the unloaded state, there be initial small crack opening Δ . Then, the value of the compressive SIF K_I^c can be determined using the expressions for the relative displacement of the crack faces v . In the case of an edge crack, we use the asymptotic solution [5]

$$v = \frac{4K_I^c}{E} \sqrt{\frac{2r}{\pi}}, \quad (5)$$

where r is the coordinate of the point on the crack surface reckoned from its tip. For internal cracks, the following approximate expression holds [5]:

$$v = \frac{4K_I^c}{E} \sqrt{\frac{2r}{\pi}} \left(1 - \frac{r}{4l}\right)$$

(l is the half-length of the internal crack). Two cases are possible in using these relations.

1. If $v_{\max} \leq \Delta$ and the crack faces are not in contact, the SIF is determined by conventional analytical or numerical methods, as in the case of extension.
2. If the value of v_{\max} calculated by formula (5) is larger than Δ , the crack faces are in contact. Then, the SIF can be determined taking into the account that, at $r = l$, the true displacement of the faces is equal to the initial opening Δ .

For edge cracks, from relation (5), we obtain

$$K_I^c = \frac{E\Delta}{4} \sqrt{\frac{\pi}{2l}}, \quad (6)$$

for internal cracks,

$$K_I^c = \frac{E\Delta}{3} \sqrt{\frac{\pi}{2l}}. \quad (7)$$

Expressions (6) and (7) are valid for a plane stress state. Accordingly, for plane deformation for an edge crack, we have

$$K_I^c = \frac{E\Delta}{4(1-\nu^2)} \sqrt{\frac{\pi}{2l}},$$

and for an internal crack,

$$K_I^c = \frac{E\Delta}{3(1-\nu^2)} \sqrt{\frac{\pi}{2l}}$$

(ν is Poisson ratio).

Thus, for compression of a solid with a crack having constant initial opening at the initiation point, the SIF value decreases with increasing length of the defect. This dependence differs from the dependence of the SIF for extension, which usually is represented as

$$K_I = Y\sigma\sqrt{\pi l},$$

where σ is the stress at a distance from the defect and Y is the shape factor of the solid.

3. Opening of a Fatigue Crack under Alternating Loading. Experimental studies of the development of fatigue cracks in metals have shown that crack closure occurs under pulsating loading [6] and that one of the main causes of this is the presence of residual plastic strain in the vicinity of the crack tip.

Let us consider the behavior of a small region of material at the crack tip, where the set of fatigue defects resulting from cyclic loading reaches the critical value, leading to material failure.

For the deformation model presented in Sec. 1, the fracture under pulsating loading corresponds to point 2 in Fig. 3, at which the tension strain is maximal. In this case, the crack extends through the examined region of the material, leading to unloading of the central rod modeling this region. A decrease in the external loading to zero results in closure of the fractures parts of the element studied, its compression, and plastic deformation; in Fig. 3, this corresponds to the segment between points 3 and 4. The extension of the system in the next loading cycle leads to elastic unloading of the fractured element, which ultimately has the total residual strain $\delta_r = 3\sigma_y c / (2E)$.

Thus, behind the tip of the growing crack there is material with positive residual strains. During unloading of the sample in each cycle, this can lead to contact interaction of the crack faces and, hence, to a decrease in the SIF amplitude.

During fatigue crack extension under symmetric loading, the deformation of the material region proceeds similarly. However, in this case, plastic deformation of the modeled region continues to the maximum value of the compressive force (point 5 in Fig. 2). A subsequent decrease in the external loading to zero leads to elastic unloading of the region studied. Finally, the examined element has the negative residual strain $\delta_r = -3\sigma_y c / E$. Hence, in this case in the absence of external load, the crack faces remain open. Residual opening of the growing fatigue crack is observed.

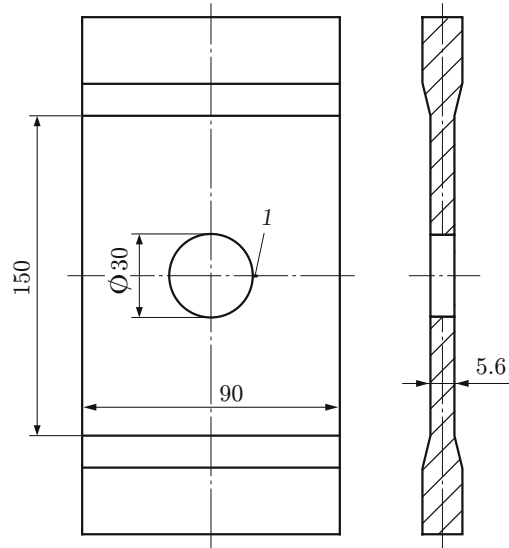


Fig. 4. Geometry and dimensions of the sample: 1 is the notch initiating a crack.

Obviously, for a certain value of the asymmetry coefficient of the cycle R , residual opening at the crack tip is absent. In the case considered, $\delta_r = 0$ for $R = \sigma_{\min}/\sigma_{\max} = -0.41$ (σ_{\max} and σ_{\min} are the maximum and minimum stresses at a distance from the crack).

If the maximum compressive load is increased by factor of two ($R = -2$), the value of δ_r increases by a factor of 3.5. Therefore, taking into account relation (2), one can assume that, for $R > -1$, the opening at the crack tip depends only on the value of the SIF K_I^c . During fatigue crack growth, the SIF K_I^c increases, reaches a maximum, and then begins to decrease (see Sec. 2). Obviously, the value of δ_r varies in the same manner. It should be taken into account that, for a constant asymmetry coefficient for the external load, the relation K_I^c/K_I^t varies.

In order for the development of a fatigue defect could be described by relations (1) or (4), the following two basic conditions should be satisfied:

- under the given external loads, the SIF amplitude (ΔK_I or $K_I^t + K_I^c$) should be larger than the threshold value;
- the crack length should be several orders of magnitude greater than the initial crack opening Δ .

Crack opening begins in the stage of crack initiation, when microdefects merge into a macrocrack. We assume that, in the stage of fatigue crack imitation, the value of Δ corresponds to the maximum value K_I^c and remains constant during the further crack growth. Then, one can assume that the initial opening of a fatigue crack under alternating loading with $R < -1$ depends only on the minimum stress of the cycle:

$$\Delta = a(\sigma_{\min})^2 \quad (8)$$

(a is a coefficient which is constant for the material studied and depends on its mechanical characteristics).

4. Analysis of Experimental Results. To verify the proposed model of crack growth, we analyzed experimental data [3].

Figure 4 shows the geometry of plates which were tested under two loading conditions: 1) $\sigma_{\max} = 47.9$ MPa and $\sigma_{\min} = -95.8$ MPa (asymmetry coefficient of the cycle $R = -2$); 2) $\sigma_{\max} = 47.9$ MPa and $\sigma_{\min} = -143.6$ MPa ($R = -3$). The samples were made of M76 rail steel with the following mechanical characteristics: conditional yield limit $\sigma_{0.2} = 510$ MPa, ultimate strength $\sigma_u = 950$ MPa, relative rupture elongation 6%, critical and threshold values of the SIF, respectively, $K_{fc} = 35$ MPa \cdot m^{1/2} and $K_{th} = 6$ MPa \cdot m^{1/2}.

A fatigue crack was initiated by a notch made on one side of the central hole (Fig. 4). For each loading regime, the crack length was measured in steps for a specified number of cycles. The measurement results are shown by points in Fig. 5.

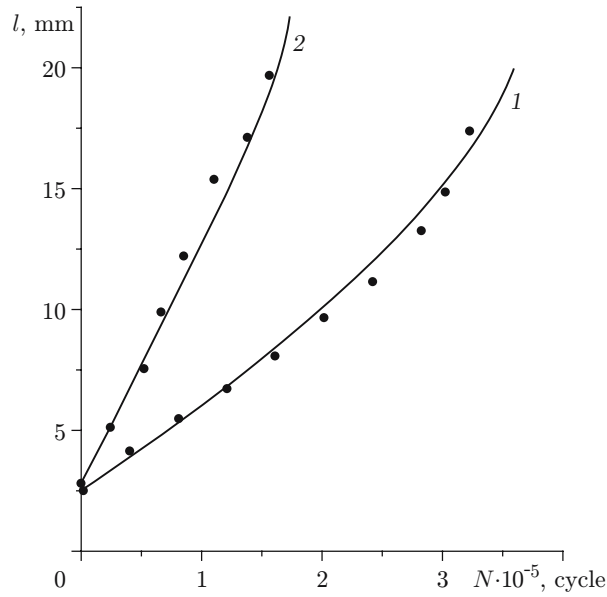


Fig. 5. Fatigue crack length versus number of loading cycles: points correspond to experimental data [3], and curves to calculation results; 1) crack development in the first loading regime; 2) the same for the second regime.

It has been noted [3] that, in the case considered, the crack growth rate cannot be determined using the Paris formula, assuming that the compressive SIF is equal to zero. To validate the relations proposed above, we calculated the compressive and tensile SIFs and determined the dependence of these quantities on the crack length.

The values of K_I^t were calculated using the finite-element method [7]. Numerical modeling of the cracked sample and calculation of the corresponding SIF were performed for nine values of the crack length: 2, 5, 7, 10, 12, 15, 17, 20, and 22 mm. It was shown that the dependence of K_I^t on the crack length is most conveniently represented as a polynomial of the form

$$k = K_I^t / \sigma_{\max} = 0.671l^{0.9} - 0.702l^{1.1} + 0.192l^{1.3}, \quad (9)$$

whose coefficients were calculated using the least-squares method. In this expression, in order for the value of SIF k to be in meters to a power of 1/2, the crack length should be in millimeters.

The results of the numerical calculation were used to analyze the dependence of the crack face displacement v on the coordinate r . The maximum difference between the calculated values v (at $r = l$) and the crack opening determined from the asymptotic solution (5), was 3% for $l = 10$ mm and 6% for $l = 20$ mm. This allowed us to use expression (6) to determine the value of SIF K_I^c . The initial opening of the fatigue crack Δ included in this relation was calculated by formula (8).

Next, from experimental data (Fig. 5), we determined the average rate of crack propagation in each step of the measurements. These results were approximated by dependence (4) using the least-squares method. Relations (6), (8), and (9) were used to find the values of the constants C , m , and a : $C = 1.18 \cdot 10^{-10}$, $m = 4.41$, and $a = 1.22 \cdot 10^{-10} \text{ m/MPa}^2$.

Let us compare the experimental dependences of N on l with the calculation results. Integration of expression (4) yields

$$N(l) = C \int_{l_0}^l (K_I^t(l) + K_I^c(l))^m dl,$$

where l_0 is the initial crack length for which the first measurement was performed.

Figure 5 shows curves of $N(l)$ for the two loading regimes (curves 1 and 2). It is evident that the calculated and experimental data are in good agreement.

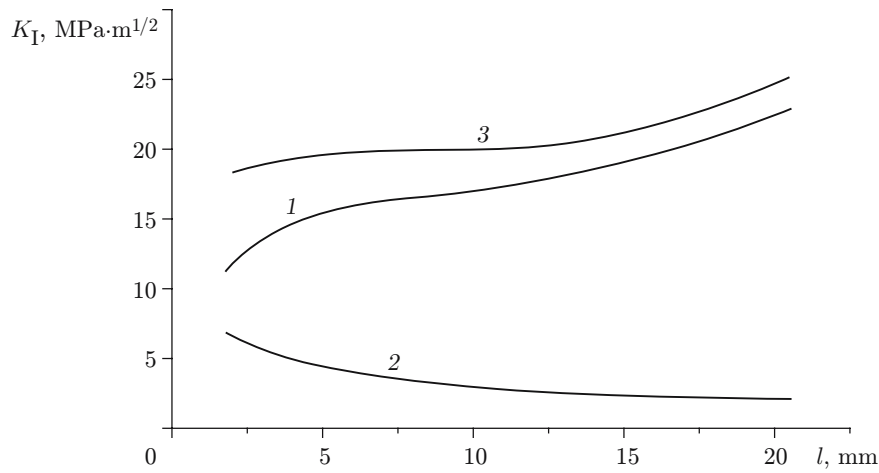


Fig. 6. The SIFs K_I^t (1), K_I^c (2), and $K_I^t + K_I^c$ (3) versus fatigue crack length for the first loading regime.

Let us check the conditions (see Sec. 3) under which relations (4) and (6) are valid. For this, we first determine the initial fatigue crack opening. According to Eq. (8), for the first loading regime, $\Delta_1 = 1.12 \cdot 10^{-3}$ mm and for the second regime, $\Delta_2 = 2.52 \cdot 10^{-3}$ mm. The length of the observed cracks is three orders of magnitude greater than the calculated value of Δ ; therefore, the cracks can be considered sharp and the SIF can be calculated using the asymptotic solution.

Let us perform a more detailed analysis of SIF values for the first loading regime. Figure 6 shows curves of K_I^c and K_I^t and their sums versus the length l . For a fatigue defect length $l > 1$ mm, the total SIF is several times larger than K_{Ith} . In this case, the total SIF $K_I^t + K_I^c$, which, according to expression (4), defines the fatigue crack growth rate, is larger than the SIF K_I^t throughout the existence of the fatigue crack, especially at an early stage of its growth. The large difference between these values indicates the need to take into account compression under alternating loading.

To estimate the effect of the compression phase on the fatigue crack growth rate, we compare the results of tests of two samples similar in geometry (see Fig. 4) under cyclic extension [3] with the data obtained. The loading parameters for the first sample are $\sigma_{\max} = 100$ MPa and $\sigma_{\min} = 20$ MPa (asymmetry coefficient $R = 0.2$), and for the second sample, they are $\sigma_{\max} = 102$ MPa and $\sigma_{\min} = 17$ MPa ($R = 0.17$).

The approximation of the measured values of the fatigue crack growth rate with relations (9) taken into account yields the following values of the coefficients in the Paris formula (1): $C = 0.78 \cdot 10^{-10}$ and $m = 4.22$.

The values of the parameters C and m are smaller than the values calculated for alternating loading. Hence, if the SIF amplitude ΔK_I is equal to the sum of the SIFs $K_I^t + K_I^c$, the fatigue crack growth rate is lower under cyclic extension than under alternating loading. It is obvious that additional fatigue defects arise in the compression half-cycle, leading to an increase in the crack growth rate compared to the growth rate in the alternating extension cycle. The difference between the rates can also be caused by crack closure (see Sec. 3).

5. Conclusions. The development of a fatigue crack under alternating loading was analyzed. The calculation results for the proposed model of elastoplastic deformation of a small region near a crack tip lead to the following conclusions:

- under alternating loading, the fatigue crack growth can be described using a relation similar to the Paris formula with the compressive SIF taken into account;
- the presence of a compression half-cycle leads to fatigue crack opening; the size of the opening depends on the loading parameters.

For compression of a cracked sample, relations for the SIF were obtained that take into account the contact of the crack faces. In this case, during crack growth, the SIF value decreases, and, hence, for relatively long fatigue cracks, the effect of the compression phase becomes less significant.

The experimental results were found to be in good agreement with the crack growth parameters calculated using the relations proposed in the present paper.

REFERENCES

1. G. Glinka, "A notch stress-strain analysis approach fatigue crack growth," *Eng. Fracture Mech.*, **21**, No. 2, 245–261 (1985).
2. J. F. Knott and J. Frederick, *Fundamentals of Fracture Mechanics*, Butterworths, London (1973).
3. L. G. Krysanov, V. P. Tyrin, and A. P. Shabanov, "Influence of compressive stresses on the development of fatigue cracks in rails," in: *Improving the Reliability of the Track Structure under Modern Operation Conditions* [in Russian], Intkest, Moscow (2000), pp. 55–59.
4. V. M. Tikhomirov and P. G. Surovin, "Extension of mixed-mode fatigue cracks in steel samples," *J. Appl. Mech. Tech. Phys.*, **45**, No. 1, 112–117 (2004).
5. V. M. Tikhomirov, "Analytical relations for displacements of a notch surface in two- and three-dimensional solids," in: *Experimental-Computational Methods for Studying Strength Problems* (collected scientific papers) [in Russian], Siberian State University of Means of Communication, Novosibirsk (2003), pp. 9–33.
6. A.S. Kobayashi (ed.), *Handbook on Experimental Mechanics*, Prentice Hall, Englewood Cliffs, New Jersey (1987).
7. M. Kh. Akhmetzyanov, V. M. Tikhomirov, and P. G. Surovin, "Determining stress intensity factors for mixed types of crack loading," *Izv. Vyssh. Uchebn. Zaved., Stroit.*, No. 1, 19–25 (2003).